

## Experimental investigation of energy dissipation properties of fibre reinforced plastics with hybrid layups under high-velocity impact loads

M. Romano <sup>a</sup>, C. Hoinkes <sup>a</sup>, I. Ehrlich <sup>a,\*</sup>, J. Höcherl <sup>b</sup>, N. Gebbeken <sup>c</sup>

<sup>a</sup> Laboratory of Composite Technology (LFT), Department of Mechanical Engineering, Ostbayerische Technische Hochschule Regensburg, Galgenbergstrasse 30, 93053 Regensburg, Germany

<sup>b</sup> Laboratory of Ballistics, Arms and Munitions, Department of Mechanical Engineering, University of the Bundeswehr Munich, Werner-Heisenberg-Weg 39, 85577 Neubiberg, Germany

<sup>c</sup> Department of Civil Engineering and Environmental Sciences, Institute of Engineering Mechanics and Structural Analysis, University of the Bundeswehr Munich, Werner-Heisenberg-Weg 39, 85577 Neubiberg, Germany

\* Corresponding e-mail address: ingo.ehrlich@oth-regensburg.de

Received 23.02.2014; published in revised form 01.05.2014

### ABSTRACT

**Purpose:** The present work deals with the experimental investigation concerning the energy dissipation capacity of different kinds of reinforcement fibres in monolithic and hybrid layups under high velocity impact loads. The investigated kinds of fibres are carbon, glass and basalt.

**Design/methodology/approach:** The test panels have been impregnated with thermoset resin. Curing was done by autoclave processing. In order to obtain comparable fibre volume contents of approx. 60 % in the different layups (monolithic and hybrid without and with separating layer), curing cycles adapted to the type of layup have been identified. The resulting fibre volume content of the test panels has been determined both by weighing and experimentally by chemical extraction and calcination. The impact load was applied by an instrumented experimental setup. Thereby both commercially available bullets and bearing balls accelerated with weighted propellant in a sabot have been used as impactors. The measured values are the velocities of the bearing balls as the impactor before and after penetration of the test panels.

**Findings:** In both cases the results show the energy dissipation capacity of each single kind of fibre in case of the monolithic layups as well as the enhanced properties of the hybrid stacked layups without and with the separating layer as a core material. Typical failure modes on the impact surface and on the outlet areas are identified.

**Research limitations/implications:** The influence of the respective kind of impactors, namely bullets and bearing balls, on the evaluated results is identified. Thereby the bearing balls exhibited a higher degree of reproducibility due to several reasons.

**Originality/value:** Fibre reinforced plastics with hybrid stacking sequences can be used as load-bearing structures and at the same time as safety structures for passengers in automotive or aerospace applications. Moreover, with the hybrid stacked composites lightweight concepts can efficiently be realized regarding energy saving issues.

**Keywords:** Fibre reinforced plastics; High velocity impact; Energy dissipation; Hybrid stacking; Autoclave processing

**Reference to this paper should be given in the following way:**

M. Romano, C. Hoinkes, I. Ehrlich, J. Höcherl, N. Gebbeken, Experimental investigation of energy dissipation properties of fibre reinforced plastics with hybrid layups under high-velocity impact loads, *Journal of Achievements in Materials and Manufacturing Engineering* 64/1 (2014) 5-19.

## PROPERTIES

### 1. Introduction

Fibre reinforced plastics are being increasingly applied in the automotive sector as well as for personal impact protection issues. Thereby especially the crash behaviour and the failure mechanisms have to be researched properly in order to ensure safety for car passengers and facilitate recovery in the crash case. Fibre reinforced plastics consisting of only one kind of reinforcement fibres under high velocity impact loads mostly fail in a brittle mode causing sharp-edged fracture surfaces and splinters.

In order to use the outstanding properties of each single kind of fibre and to avoid the afore-mentioned brittle failure modes to an optimum, the idea of using hybrid stacking sequences is adequate. Under these conditions fibre reinforced plastics with hybrid stacking sequences can be used as load-bearing structures and at the same time as safety structures for passengers in automotive or aerospace applications. Moreover, with the hybrid stacked composites lightweight concepts can efficiently be realized regarding energy saving issues.

### 2. Research environment

The research environment is the material behaviour of fibre reinforced plastics under transversal loads in the high velocity range. Therefore a brief literature review is presented. This leads to several conclusions and to the pursued mechanical principle described thereafter.

#### 2.1. Literature review

Energy dissipation mechanisms in fibre reinforced plastics are dominated by inter- and intralaminar failure modes as well as adhesive failure in the interface between

fibre and matrix. Whereas interlaminar failure means the delamination of sequent plies, intralaminar failure means fracture of fibre and matrix. Only a small amount of energy is dissipated by friction effects between fibre and matrix and plastic deformation in the polymeric matrix system. Different material parameters affect the failure modes. These are amongst others fibre orientation, fibre volume content, layup, geometry of the specimen and of the impactor as well.

Maier 1990 [5] investigated the crash-behaviour of tubular specimens with different cross-sections by experiments and finite-element-analyses. The specimens were made of glass fibre reinforced vinyl ester, poly ester and epoxy. The specimens with the epoxy matrix system exhibited the highest energy dissipation capacity. Additionally the influence of the processing and the geometry on the energy dissipation capacity has been investigated.

Morita et al. 1997 [7] characterized the damage tolerance of fibre reinforced plastics under high velocity impact loads with a varied degree of anisotropy. Thereby the degree of anisotropy means the change of fibre orientation for sequent layers in the layup. The results showed an enhanced energy dissipation capacity with an increased degree of anisotropy for sequent layers in the layup. Simultaneously the damage area in terms of interlaminar delaminations increased.

Holmquist and Johnson 2002 and 2005 [3,2] investigated the reaction of silicone carbide to transversal impact loads in the high velocity range. The investigated material is a ceramic. The originally high energy dissipation capacity could even be enhanced by creating predefined residual stresses, suited to the specific material properties.

Muhi, Najim and Moura 2009 [9] considered the effect of hybridization of glass fibre reinforced plastics with single layers of aramid fabrics under transversal high velocity impact. Therefore five kinds of different layups

have been investigated experimentally. These are a monolithic layup consisting of only four layers of glass fabrics and in comparison four hybrid layups where at different positions in the layup one layer of glass fabric is substituted by one layer of aramid fabric (Kevlar 29) at a time. Additionally three different geometries of the impactor have been used. As a completion analytical approaches following Morye et al. 2000 [8] have been carried out. The hybridization in terms of substituting one layer of glass fabric with one layer of aramid fabric yields enhanced penetration resistance as well as sensitivity to the position of the hybrid substitute layer in the construction of the layup. In detail the hybridized layup where the opposite impact side has been substituted exhibits the highest energy dissipation properties.

Fadhel 2011 [1] carried out finite-element-analyses for pure polycarbonate specimens under high velocity impact loads varying their thickness. Additionally two different geometries for the impactor have been investigated. Even though the work is focused on pure polymeric materials the essential conclusion of the simulations is that an enhanced elastic sag could be identified as the main reason for an increasing dissipated energy.

Melo and Villena 2012 [6] investigated the influence of the fibre volume content on the energy dissipation capacity of fibre reinforced plastics. For glass fibre reinforced plastics with epoxy, polyester and vynilester matrix systems higher values of the fibre volume content in the specimens yield significantly higher energy dissipation properties. Additionally the materials with epoxy matrix system exhibited the highest energy dissipation capacity.

Rosenberg and Dekel 2012 [22] basically describe the experimental setup and procedure as well as the evaluation of the experimentally determined results when transversal impact tests in the high velocity range are considered.

## 2.2. Pursued mechanical principle

The object in the carried out investigations is the identification of the energy dissipation capacity of fibre reinforced plastics under high velocity impact loads. Thereby besides monolithic layups selected hybrid layups with and without separating layer are investigated. The aim is to enhance the energy dissipation capacities by hybrid layups based on fabrics of different kinds of fibre reinforcements besides using the outstanding material properties of fibre reinforced plastics as load bearing structures. Therefore two basic ideas are followed.

### Hybrid stacking sequences

As a first approach the use of hybrid stacked layups instead of monolithic layups is relatively simple. Thereby the characteristic properties of carbon and glass fibres, completed by basalt fibres, respectively, can be used through the thickness by reasonably defined hybrid stacking sequences.

### Separating layers as elastic support

A second approach is the use of separating layers as a core material. Here, especially comparatively thin separating layers with relatively low stiffness are used. In the present application, however, it is not used with the aim of enhancing the moment of inertia as usually done. In contrast the used separating layers with the afore described properties provide an elastic support and a shear plane for the single layers in the layup. Thereby transversal loads can increasingly be transferred to in-plane loads.

This effect is reached by additionally providing transversal deflection due to shear effects and therewith enhances the resulting in-plane loads in the material as exemplarily demonstrated in Jones 2009 [4]. The reason for this pursued principle is, that fibre reinforced plastics show their outstanding properties under in-plane tensile loads in direction of the reinforcement fibres. The aim is to reduce the effect of plugging the material by the impactor but enable the afore described structural mechanic effects similarly to Fadhel 2011 [1].

### Limit of the experimental investigations

With the afore described basic ideas the initial situation for using the light-weight properties of fibre reinforced plastics as well as enhance their resistance to transversal impact loads in the high velocity range can be created. These two basically different properties enable the application of fibre reinforced plastics as load-bearing structure and at the same time as protective structure. If thereby for load-bearing structures additional protective structures can be omitted, a holistic light-weight approach can be achieved.

Alternative approaches for enhancing the resistance of fibre reinforced plastics under transversal impacts in the high velocity range by the impact resistance of the matrix, i.e. by definably adding small amounts of thermoplastics to the thermoset matrix system is not the aim of the carried out investigations. They are merely focused on the material suited or fibre suited application of different kinds of reinforcement fibres in hybrid stacked layups, respectively.

## 2.3. General experimental conditions

Knowing that different layer orientations have influence on the energy dissipation capacity [7] all test panels have

been built up with a  $[(0/90)_n]$  orientation. This was done as a first attempt for characterizing the general material behaviour. The fibre volume content is a significant parameter for the quality and reproducibility of fibre reinforced plastics [24,25]. Moreover it has a massive influence on the energy dissipation capacity [6].

In order to experimentally investigate the specific capacities of monolithic and hybrid stacking sequences regarding energy dissipation high velocity impact tests have been carried out. Thereby both commercially available bullets of the kind 9 mm Luger [12] and bearing balls [11] accelerated with weighted propellant in a sabot have been used as impactors. The bullets weighting approx. 8.96 g reached velocities of approx. 228 m/s so that the kinetic energies are approx. 225 J. The bearing balls of steel weighting approx. 1.12 g have been accelerated to average velocities of 560 m/s yielding kinetic energies of approx. 176 J. The measured values are the velocities of the bearing balls as the impactor before and after penetration of the test panels.

Evaluation of the experimentally obtained results for the velocities of the impactor before and after penetration according to Rosenberg and Dekel 2012 [22] provides information about the capacity for each single stacking sequence to dissipate kinetic energy. Confronting the evaluated results the influence of the respective kind of impactors, namely bullets and bearing balls, can be identified with respect to reproducibility and validity.

### 3. Materials and test procedures

In the following used materials and the material processing is described. The experimental equipment used to determine the fibre volume content and the energy dissipation capacity are mentioned. The respective standards (DIN, EN or ISO) are indicated.

#### 3.1. Materials and processing

For the processing of the test panels three different kinds of reinforcement fibres, namely carbon, glass and basalt fabrics, have been used. In each case a twill weave 2/2 has been used as a textile semi-finished product for further processing and building-up the selected layups. An additional hexagonal core material is of the kind Lantor Soric XF [20]. It is used as a hexagonal separating layer. This separating layer aims at an enhanced sag of the test panels [4], which should dissipate more energy when penetrated [1]. Its initial thickness is approx. 4 mm. Due to

the applied pressure in the later described autoclave curing process its thickness reduces to approx. 1 mm.

The single fabric reinforced layers have manually been pre-impregnated. This process enables the choice of a selected thermoset resin. Thereby for the first set of specimens the medium viscous 120 °C bisphenol A epoxy resin of the kind Epikote Resin 05128 [18] and for the second set the anhydrid 180°C warm curing epoxy resin Epikote Resin 04572 [17] were chosen. The curing was done in an autoclave process under a vacuum bag according to the process indicated in the data sheet of the respective matrix system [18,17].

Table 1 lists the two sets of produced test panels with the respective labelling, stacking sequence and matrix system, number of single layers and fibre volume content  $\varphi_f$ . As later described in Section 3.4 the first set of specimens has been impacted by commercially available bullets as impactors whereas the second set of specimens has been impacted by bearing balls accelerated with weighted propellant in a sabot. Thereby the determination of the fibre volume content as a characteristic indicator for the mechanical quality of the material is briefly described in the following Section 3.2. There are three kinds of monolithic layups consisting of only carbon, glass and basalt fabric reinforced layers. Additionally there is one hybrid layup in the first set of specimens and two kinds of hybrid layups in the second set of specimens, each one consisting of carbon, glass and basalt. The two hybrid layups in the second set of specimens distinguish from each other by the afore mentioned additionally added hexagonal separating layer Lantor Soric XF [20] as a core material. Its areal weight is 240 g/m<sup>2</sup>. Its position is after the first twelve fabrics or before the last four fabrics, respectively, considering the direction of the later impact.

With the afore indicated parameters a thickness of approx. 4 mm and a fibre volume content of approx. 60% of all investigated test panels have been achieved. In order to reach a constant thickness of the test panels the number of single layers in each layup has to be adopted due to the varying thicknesses of the fabrics.

The geometric dimensions have been selected following DIN 65561 [14]. The German standard requires a final lateral geometry of the specimens of 150 mm x 100 mm. The panels have been built up with a dimension of 210 mm x 160 mm since the edges of the test panels become inhomogeneous and unsteady. The edges have then been cut off by water jet cutting. Specimens for the experimental determination of the fibre volume content  $\varphi_f$  have been cut off from the cut-off regions near the cutting edge. Their dimensions are approx. 15 mm x 15 mm according to DIN EN ISO 1172 [15] and DIN EN 2564 [16], respectively.

Table 1.

Labelling, types of fabrics, respective matrix system, stacking sequences, number of layers and fibre volume content  $\varphi_f$  of the two different sets of comparable specimens: First set  $C_1$  (carbon),  $G_1$  (glass),  $B_1$  (basalt) and  $G+C+B_1$  impacted by commercially available bullets. Second set  $C_2$  (carbon),  $G_2$  (glass),  $B_2$  (basalt),  $C+G+B_2$  and  $C+G+Hex+B_2$  impacted by bearing balls accelerated with weighted propellant in a sabot

ID	Material	Type of fabric	Areal weight	Matrix system	Stacking sequence	Number of layers	Curing Temp.	Fibre vol. content $\varphi_f$	Literature
$C_1$	mono-lithic	twill 2/2	245 g/m <sup>2</sup>	Epikote Resin 05128	$[(0/90)_{18}^C]$	18	120 °C	62.02%	[13,18]
$G_1$	mono-lithic	twill 2/2	280 g/m <sup>2</sup>	Epikote Resin 05128	$[(0/90)_{18}^G]$	18	120 °C	55.96%	[18,19]
$B_1$	mono-lithic	twill 2/2	345 g/m <sup>2</sup>	Epikote Resin 05128	$[(0/90)_{18}^B]$	18	120 °C	63.37%	[10,18]
$G+C+B_1$	hybrid	-	-	Epikote Resin 05128	$[(0/90)_4^G/(0/90)_4^C/(0/90)_8^B]$	16	120 °C	58.52%	[10,13,18,19]
$C_2$	mono-lithic	twill 2/2	245 g/m <sup>2</sup>	Epikote Resin 04572	$[(0/90)_{18}^C]$	18	180 °C	63.60%	[13,17]
$G_2$	mono-lithic	twill 2/2	280 g/m <sup>2</sup>	Epikote Resin 04572	$[(0/90)_{18}^G]$	18	180 °C	58.65%	[17,19]
$B_2$	mono-lithic	twill 2/2	345 g/m <sup>2</sup>	Epikote Resin 04572	$[(0/90)_{18}^B]$	18	180 °C	61.16%	[10,17]
$C+G+B_2$	hybrid	-	-	Epikote Resin 04572	$[(0/90)_4^C/(0/90)_4^G/(0/90)_8^B]$	16	180 °C	63.07%	[10,13,17,19]
$C+G+Hex+B_2$	hybrid + separating layer	-	-	Epikote Resin 04572	$[(0/90)_4^C/(0/90)_4^G/(0/90)_4^B/(Hex)_1/(0/90)_4^B]$	16+1	180 °C	57.15%	[10,13,17,19,20]

In order to achieve a statistically secured amount of comparable specimens five test panels have been produced for each selected layout, so that a total number of 55 specimens (20 specimens of the first set and 25 specimens of the second set) have been investigated.

### 3.2. Determination of the fibre volume content

Basically there are two methods for experimentally investigating the fibre volume content. Whereas for inorganic fibres like glass or basalt fibres it can be determined by thermal vaporization the polymeric matrix system according to DIN EN ISO 1172 [15,23], for organic fibres like carbon fibres it can be determined by chemical

extraction of the fibres according to DIN EN 2564 [16]. For a statistically ensured determination five specimens of every test panel with geometric dimensions of approx. 15 mm x 15 mm have been investigated. In both cases knowing the mass of the initial specimen and the remaining fibres as well as the densities of the single components, namely fibre and matrix, it is possible to determine the fibre volume content  $\varphi_f$ .

Table 1 contains the results of the determination of the fibre volume content  $\varphi_f$  of the single kinds of test panels. The relatively high values of the fibre volume content show high mechanical quality of the material. The relatively low standard deviations represent a high degree of reproducibility of the process at the same time.

### 3.3. Experimental setup for high velocity impact tests

In order to carry out and properly evaluate the high-velocity impact tests an adequate experimental setup of test equipment is necessary. The experimental setup is schematically shown in Figure 1a. It consists of:

- an instrumented barrel for acceleration of the impactor on the target,
- two photoelectric barriers for determining the velocity of the impactor before the impact,
- a test panel mounting where the specimens are inserted and clamped all around with eight bolts M8, each tightened with 5 Nm,
- a double exposure instrumentation with the respective high-speed photographic camera for determining the velocity of the impactor after penetration of the target,
- a bullet screen and a fire case for absorbing the impactor and fragments that have possibly been released.

The measured values are the velocities of the impactors before and after the penetration of the material. On the ballistic flight of the impactor the photoelectric barrier provides the velocity of the impactor before the impact  $v_1$ , the impactor hits the target and after penetration the double exposure with the high-speed camera provides the velocity of the impactor after the penetration  $v_2$ . Figure 1b

exemplarily shows an image of the high-speed camera after the impactor has penetrated the material. Due to the double exposure the impactor is pictured twice. Knowing the time between the two exposures and measuring the distance between the two pictured impactors on the image allows the calculation of the velocity of the impactor after the penetration  $v_2$ .

### 3.4. High velocity impact tests with bullets and bearing balls as two kinds of impactors

The impact load was applied by the afore described instrumented experimental setup. In detail for the first set of specimens commercially available bullets have been used as impactors whereas for the second set of specimens bearing balls in a sabot accelerated with weighted propellant have been used as impactors. This variation of parameters enables the identification of the influence of the impactor on the experimentally determined energy dissipation properties of the investigated materials.

In detail the bullets are of the kind 9 mm Luger [12]. They weigh approx. 8.96 g and reached velocities before the impact of approx. 228 m/s so that the kinetic energies are approx. 225 J. Figure 2a shows a schematic lateral view of the cartridge with its geometric dimensions in millimetres.

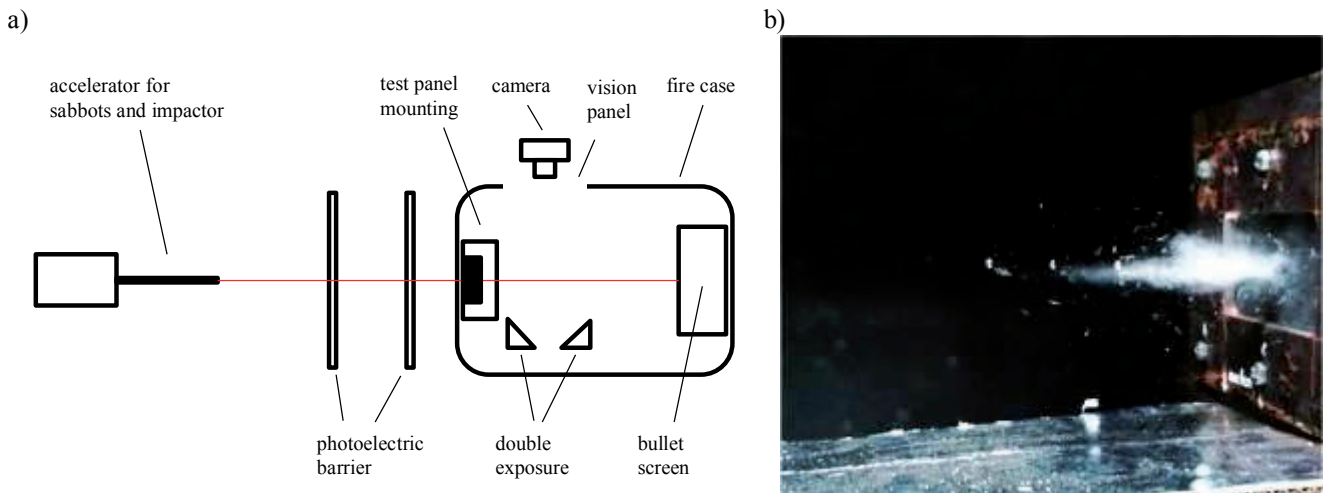


Fig. 1. Schematic illustration of the experimental setup for high velocity impact tests (a) and high-speed image of the debris after penetration under double exposure (b)

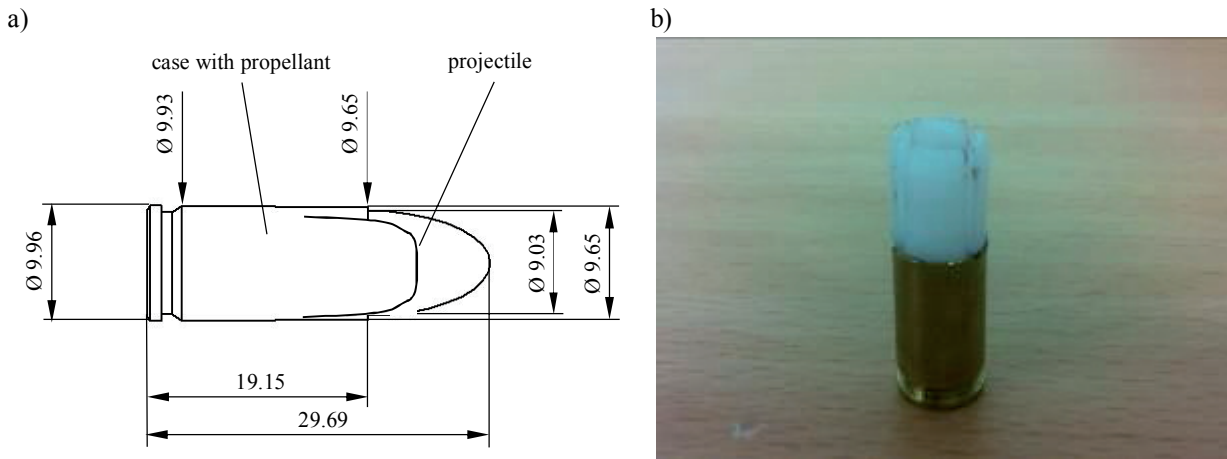


Fig. 2. Schematic lateral view of the cartridge of the kind 9 mm Luger [12] (a) and CNC-manufactured plastic sabot made of Polyoxymethylen (POM) [21] with the mounted case containing precisely weighted propellant (b)

Table 2.

Material, nominal diameter, mass of the impactor  $m$ , velocity before penetration  $v_1$  and corresponding initial kinetic energy  $E_{kin,1}$  for both kinds of impactors used for the two different sets of investigated kinds of layouts

Kind of impactor	Material	Nominal diameter	Mass $m$	Initial velocity $v_1$	Initial kinetic energy $E_{kin,1}$
Bullet 9 mm Luger [12]	-	9 mm	$8.96 \pm 0.0188$ g	$288.2 \pm 6.8 \frac{m}{s}$	$3722 \pm 17.8$ J
Bearing ball [11]	100Cr6 steel	6.5 mm	$1.12 \pm 0.0005$ g	$560.3 \pm 5.8 \frac{m}{s}$	$175.8 \pm 3.7$ J

The bearing balls of steel weighting approx. 1.12 g have been accelerated to average velocities of 560 m/s yielding kinetic energies of approx. 176 J. The bearing balls are of the steel type 100Cr6 [11]. With a diameter of 6.5 mm and the corresponding density of 7.61 g/cm<sup>3</sup> the impactors have a mass of 1.12 g. Computer numerically controlled (CNC) manufactured plastic sabots made of Polyoxymethylen (POM) [21] as shown in Figure 2b have been used to accelerate the bearing balls in a barrel. The case on which the plastic sabot is mounted is filled with a special propellant, which was weighted to 0.1 mg precision in order to properly accelerate the impactor in the barrel after ignition. The afore described procedure provides reproducible velocities of the impactor after having left the barrel [22].

### 3.5. Evaluation of experimental results

For the evaluation of the experimental investigation each impactor is weighted to 0.1 mg precision. Knowing the velocity of the impactor before the impact provided

by the photoelectric barrier  $v_1$  and the velocity of the impactor after penetration of the material provided by the double exposure and the high-speed camera  $v_2$  the kinetic energy for both states can be calculated by

$$E_{kin,n} = \frac{1}{2} m v_n^2, \quad (1)$$

where  $m$  is the mass,  $v$  is the velocity and  $n$  indicates the states, 1 before and 2 after penetration of the material. Table 2 contains the nominal diameter and mass of the impactor as well as the velocity before penetration and the corresponding initial kinetic energy for both kinds of impactors in terms of mean value and standard deviation.

The difference between the kinetic energies before the impact  $E_{kin,1}$  and after penetration of the material  $E_{kin,2}$  allows calculating the absolute value for the dissipated energy by penetrating the material by [22]

$$E_{diss} = \Delta E_{kin} = E_{kin,1} - E_{kin,2} = \frac{1}{2} m (v_1^2 - v_2^2). \quad (2)$$

In order to properly evaluate each single test and achieve nondimensional comparable results for the carried out experimental investigations it is reasonable to introduce the relative dissipated kinetic energy [22]

$$E_{\text{diss,rel}} = \frac{\Delta E_{\text{kin}}}{E_{\text{kin},1}} = \frac{\frac{1}{2} m (v_1^2 - v_2^2)}{\frac{1}{2} m v_1^2} = \frac{v_1^2 - v_2^2}{v_1^2} = 1 - \frac{v_2^2}{v_1^2}, \quad (3)$$

where the dissipated kinetic energy due to penetration of the material  $\Delta E_{\text{kin}}$  is related to the initial kinetic energy of the impactor  $E_{\text{kin},1}$ . The introduction of the relative dissipated kinetic energy  $E_{\text{diss,rel}}$  provides a specific value in percent. It indicates the capacity of a material to dissipate kinetic energy applied by high velocity impacts when the material gets penetrated.

The experimentally determined fibre volume contents  $\varphi_f$  vary in a range of 56% to 63%. The distinct variation exists even though the same manufacturing process described before as well as the same autoclave curing cycle has been used. That is the reason why the former described evaluation of the relative dissipated kinetic energy  $E_{\text{diss,rel}}$  has to be evaluated additionally. In order to achieve completely comparable values the further calculated ones based on the nominal values are standardized. Therefore the relative dissipated kinetic energy  $E_{\text{diss,rel}}$  is standardized to a constantly presumed fibre volume content  $\varphi_{f,s}$  by calculating

$$E_{\text{diss,rel}}(\varphi_{f,s}) = E_{\text{diss,rel}} \frac{\varphi_{f,s}}{\varphi_{f,e}}, \quad (4)$$

where the subscripts s and e indicate the desired standardized value for the fibre volume content and the experimentally determined fibre volume content listed in Table 1, respectively. As already mentioned before the applied pressure in the autoclave curing cycle was modified in order to achieve a fibre volume content of approx. 60%. Therefore the presumed fibre volume content for the standardization is selected to  $\varphi_{f,s} = 60\%$ .

## 4. Results and discussion

In the following the evaluation of the experimental results is described. The obtained results are discussed and lead back to acting effects.

Figure 3 graphically illustrates the relative dissipated kinetic energy  $E_{\text{diss,rel}}$  of each selected type of layup calculated by equation (3) of the two different sets of comparable specimens. Figure 4 graphically illustrates the relative dissipated kinetic energy  $E_{\text{diss,rel}}(\varphi_{f,s} = 60\%)$  of each selected type of layup calculated by equation (4) as standardized results of the two different sets of comparable specimens. Table 3 finally resumes the results of the investigated kinds of layups of the two sets of comparable specimens in terms of mean value and standard deviation.

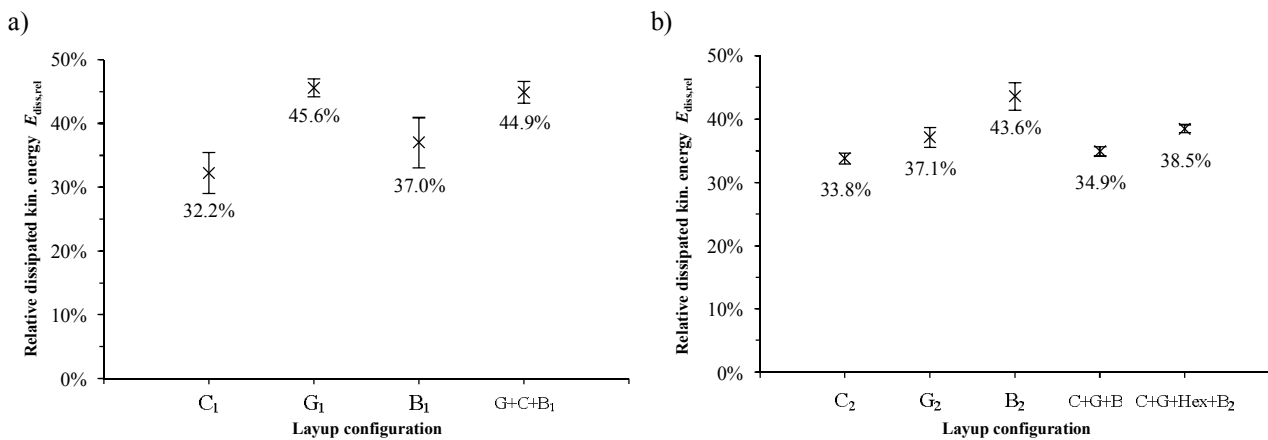


Fig. 3. Relative dissipated kinetic energy  $E_{\text{diss,rel}}$  of the monolithic and hybrid materials based on the absolute values of the fibre volume content  $\varphi_{f,e}$ ; a) results of the first set of the investigated kinds of layups C<sub>1</sub> (carbon), G<sub>1</sub> (glass), B<sub>1</sub> (basalt) and G+C+B<sub>1</sub> impacted by commercially available bullets; b) results of the second set of the investigated kinds of layups C<sub>2</sub> (carbon), G<sub>2</sub> (glass), B<sub>2</sub> (basalt), C+G+B<sub>2</sub> and C+G+Hex+B<sub>2</sub> impacted by bearing balls accelerated with weighted propellant in a sabot

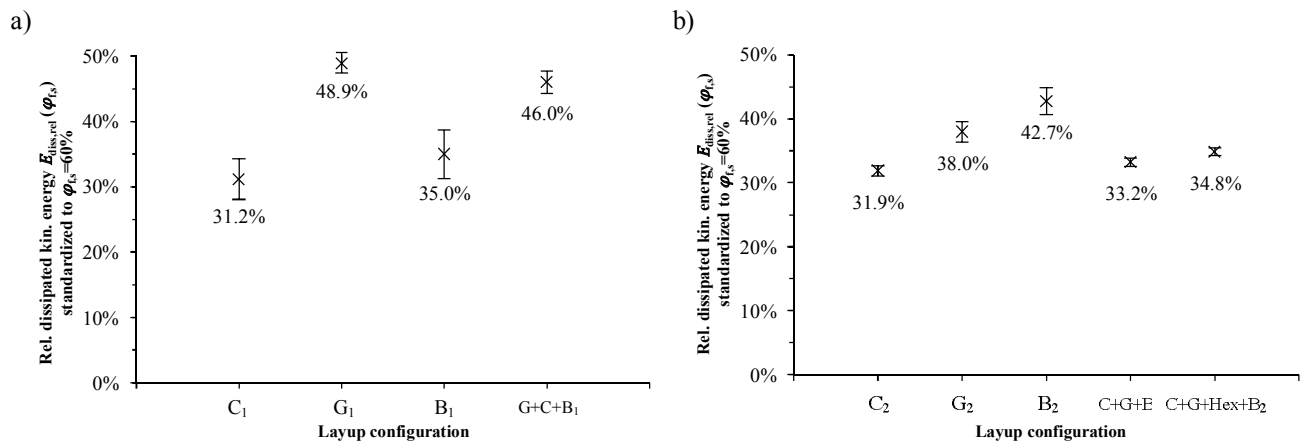


Fig. 4. Relative dissipated kinetic energy  $E_{diss,rel}(\varphi_{f,s})$  of the monolithic and hybrid materials standardized to a fibre volume content  $\varphi_{f,s} = 60\%$ ; a) results of the first set of the investigated kinds of layups C<sub>1</sub> (carbon), G<sub>1</sub> (glass), B<sub>1</sub> (basalt) and G+C+B<sub>1</sub> impacted by commercially available bullets; b) results of the second set of the investigated kinds of layups C<sub>2</sub> (carbon), G<sub>2</sub> (glass), B<sub>2</sub> (basalt), C+G+B<sub>2</sub> and C+G+Hex+B<sub>2</sub> impacted by bearing balls accelerated with weighted propellant in a sabot

Table 3.

Relative dissipated kinetic energy  $E_{diss,rel}$  and standardized relative dissipated kinetic energy  $E_{diss,rel}(\varphi_{f,s} = 60\%)$  of the investigated kinds of layups of the two different sets of specimens in terms of mean value and standard deviation: First set C<sub>1</sub> (carbon), G<sub>1</sub> (glass), B<sub>1</sub> (basalt) and G+C+B<sub>1</sub> impacted by commercially available bullets. Second set C<sub>2</sub> (carbon), G<sub>2</sub> (glass), B<sub>2</sub> (basalt), C+G+B<sub>2</sub> and C+G+Hex+B<sub>2</sub> impacted by bearing balls accelerated with weighted propellant in a sabot

ID	Kind of impactor	Relative dissipated kinetic energy $E_{diss,rel}$	Standardized relative dissipated kinetic energy $E_{diss,rel}(\varphi_{f,s} = 60\%)$
C <sub>1</sub>	Bullet 9 mm Luger [12]	32.2 ± 3.2%	31.2 ± 3.1%
G <sub>1</sub>		45.6 ± 1.4%	48.9 ± 1.5%
B <sub>1</sub>		37.0 ± 4.0%	35.0 ± 3.8%
G+C+B <sub>1</sub>		44.9 ± 1.7%	46.0 ± 1.7%
C <sub>2</sub>	Bearing ball [11]	33.8 ± 0.9%	31.9 ± 0.8%
G <sub>2</sub>		37.1 ± 1.6%	38.0 ± 1.6%
B <sub>2</sub>		43.6 ± 2.2%	42.7 ± 2.1%
C+G+B <sub>2</sub>		34.9 ± 0.7%	33.2 ± 0.7%
C+G+Hex+B <sub>2</sub>		38.5 ± 0.7%	34.8 ± 0.6%

In each case the relative dissipated kinetic energy  $E_{diss,rel}$  and the standardized relative dissipated kinetic energy  $E_{diss,rel}(\varphi_{f,s})$  to the desired value of the fibre volume content  $\varphi_{f,s} = 60\%$  vary only slightly. Because the initial values of the fibre volume content  $\varphi_{f,e}$  do not

distinctly differ from the desired value of the fibre volume content  $\varphi_{f,s} = 60\%$ , as indicated in Table 1, the tendencies are similar to the results obtained for the nominal values. Because the standard deviations are standardized as well, the tendencies in the results based on the nominal values do not change.

#### 4.1. Results based on the nominal values of the fibre volume content $\varphi_{f,e}$

The relative dissipated kinetic energy of the first set of investigated specimens consisting of monolithic layups containing only a single kind of reinforcement fibre, illustrated in Figure 3a, ranges from 32% to 46%. The highest value of the relative dissipated kinetic energy of approx. 46% is obtained for the test panels built up of only glass fabrics. The test panels consisting of only basalt fabrics dissipated approx. 37% whereas the test panels containing only carbon fabrics dissipated approx. 32% of the initial impact energy. The standard deviation ranges from 1.4% to 4.0%. Thereby the glass fibre reinforced test panels showed the lowest standard deviation in contrast to the basalt fibre reinforced specimens that showed the highest values. The relative dissipated kinetic energy of the test panels consisting of the hybrid layup is 45%. In contrast to the monolithic materials the hybrid stacked layup showed a relatively low standard deviation.

The relative dissipated kinetic energy of the second set of investigated specimens consisting of monolithic layups containing only a single kind of reinforcement fibre, illustrated in Figure 3b, range from 34% to 44%. The highest value of the relative dissipated kinetic energy of approx. 44% is obtained for the test panels built up of only basalt fabrics. The test panels consisting of only glass fabrics dissipated approx. 37% whereas the test panels containing only carbon fabrics dissipated approx. 34% of the initial impact energy. The standard deviation is persistently low and lies in a range of 0.85% to 2.2%. Thereby the carbon fibre reinforced test panels showed the lowest standard deviation in contrast to the basalt fibre reinforced specimens that showed the highest values. The relative dissipated kinetic energy of the test panels consisting of the hybrid layups with and without the hexagonal separating layer range from 35% to 39%. Confronting the hybrid stacked layup without hexagonal separating layer and the hybrid stacked layup with hexagonal separating layer as a core material a distinct effect can be noticed. The hybrid stacked material with separating layer shows approx. 4% higher values for the relative dissipated kinetic energy than the hybrid stacked layup without separating layer. In contrast to the monolithic materials the hybrid stacked materials showed the lowest standard deviation.

#### 4.2. Standardized experimental results to a fibre volume content $\varphi_{f,s} = 60\%$

The standardized relative dissipated kinetic energy  $E_{\text{diss,rel}}(\varphi_{f,s})$  of the monolithic materials of the first set of investigated materials, illustrated in Figure 4a, range from 31% to 49%. The highest value of approx. 49% is obtained for the test panels built up of only glass fabrics. To the test panels consisting of only basalt fabrics a value of approx. 35% is assigned. For the monolithic carbon fibre reinforced layups the standardization yields a value of approx. 31%. The hybrid stacked specimens yield a value of 46%.

The standardized relative dissipated kinetic energy  $E_{\text{diss,rel}}(\varphi_{f,s})$  of the monolithic materials of the second set of investigated materials, illustrated in Figure 4b, ranges from 32% to 43%. The highest value of approx. 43% is still obtained for the test panels built up of only basalt fabrics. To the test panels consisting of only glass fabrics a value of approx. 38% is assigned. For the monolithic carbon fibre reinforced layups the standardization yields a value of approx. 32%. When the values of the hybrid stacked materials are considered, they range from 33% to 35%. Because the initial values of the fibre volume content  $\varphi_{f,e}$  do not distinctly differ from the desired value of the fibre volume content  $\varphi_{f,s} = 60\%$  the tendencies are similar to the results obtained for the nominal values 33% for the hybrid layup without hexagonal core material and 35% for the hybrid layup with hexagonal core material. However, the effects caused by the separating layer used as a core material are a little less distinct, yet clearly observable. The hybrid stacked material with separating layer shows approx. 2% higher values for the standardized relative dissipated kinetic energy than the hybrid stacked layup without separating layer.

#### 4.3. Description of failure modes – impact surface and outlet areas

In the following the characteristic failure modes of the different kinds of layups of the two investigated sets of specimens are confronted with each other. Therefore the fractured surfaces of the impact side as well as of the opposite side are described. Whereas Figure 5 shows the characteristic fractures surfaces of the penetrated specimens of the first set of investigated materials, Figure 6 exemplarily shows them for the second set of investigated specimens. Thereby the top row shows the fractured surfaces on the impact side and the bottom row shows them on the opposite side. As in each case the relevant area is illustrated a scale of 10 mm is indicated.

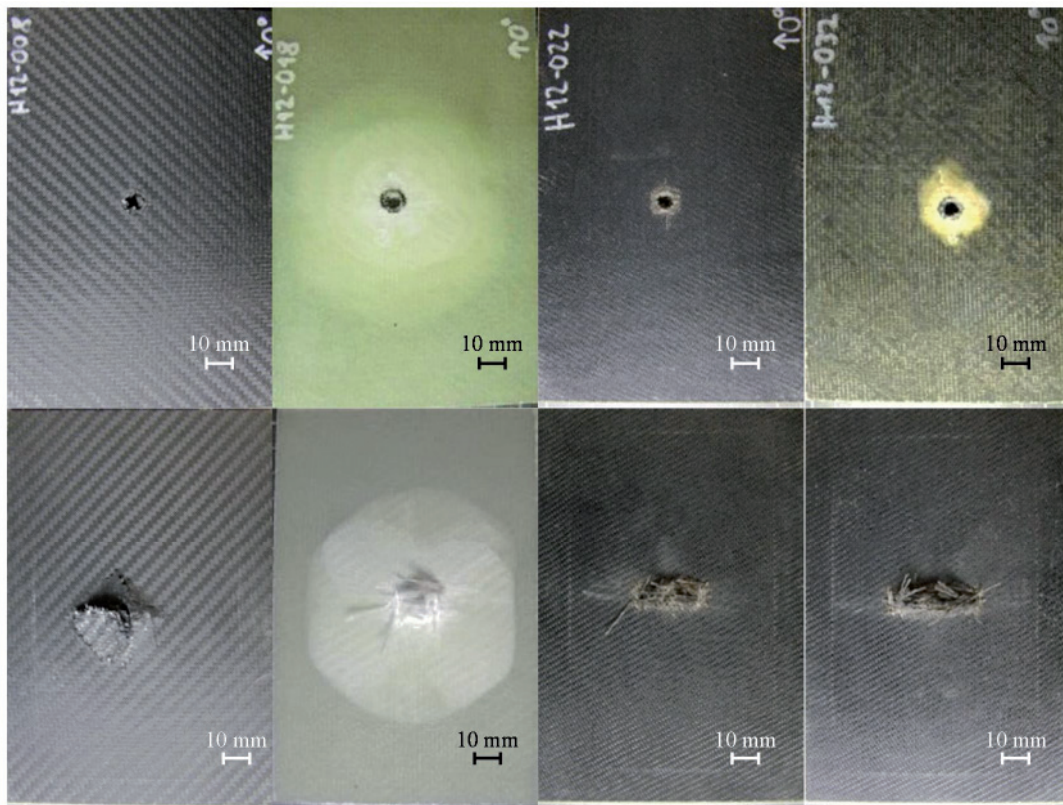


Fig. 5. Characteristic failure modes of the first set of investigated kinds of layups: From left to right:  $C_1$  (carbon),  $G_1$  (glass),  $B_1$  (basalt) and  $G+C+B_1$  (Top row: Impact side, Bottom row: Opposite impact side)

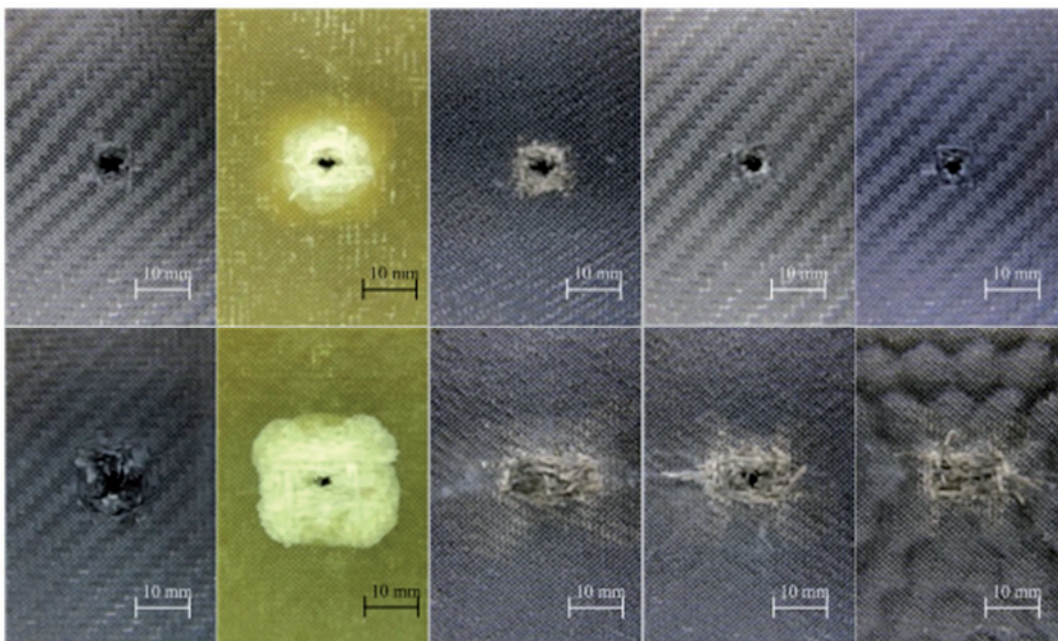


Fig. 6. Characteristic failure modes of second set of investigated kinds of layups: From left to right:  $C_2$  (carbon),  $G_2$  (glass),  $B_2$  (basalt),  $C+G+B_2$  and  $C+G+Hex+B_2$  (Top row: Impact side, Bottom row: Opposite impact side)

For both sets of investigated specimens the specimens that only contain carbon fibres show a distinct contour on the impact side. This can be interpreted as a die-cutting or plugging effect because of the relatively high stiffness of the carbon fibre reinforced material. On the opposite side a partially very splinted surface due to brittle fracture can be observed. Due to the typical opaque property for carbon fibre reinforced plastics interlaminar delaminations are not visible yet existing.

In contrast, for the glass fibre reinforced specimens of both sets of investigated specimens the interlaminar delaminations are recognizable due to the transparency of both the fibres and the matrix system. On the opposite side of the impact for both investigated kinds of specimens a clearly outlined delamination area can be identified between the last two single layers. This area is distinctly larger regarding the first set of specimens. In this case the boundary effect near the edges of the test panel mounting can be observed. Comparing the delamination areas on the impact side to the area on the opposite side a conical spreading of the delamination areas through the thickness can be assumed. Due to the  $[(0/90)_n]$  layups with equilibrated twill fabrics and the rectangular form of the free part of the specimen in the test panel mounting the delamination has a slightly rectangular shape, too, when the second set of investigated specimens is addressed.

For the basalt fibre reinforced material the interlaminar delaminations are not clearly identifiable due to the opaque optical properties of basalt fibres. Confronted to the glass fibre reinforced material the interlaminar delaminations on the opposite side of the impact can slightly be discerned for both sets of investigated kinds of layups. Because of the slightly unbalanced construction of the basalt fabric the delamination on the opposite side of the impact is distinctly rectangular.

The contour on the impact side of the hybrid layups of both sets of investigated kinds of layups without separating layer are similar to the contours of the specimens that only contain carbon fibre reinforcement. On the opposite side of the impact the basalt fabrics cause a fine extensive fractured surface. On the opposite side of the impact the interlaminar delamination between the last single layers of basalt fabrics can slightly be discerned.

Regarding the hybrid layups with separating layer of the second set of investigated kinds of layups the contour due to the penetration on the impact side is shaped like the ones of the hybrid layups without separating layer or the purely carbon fibre reinforced material. On the opposite side of the impact the hexagonal structure of the core material is

slightly visible. The fractured area can be identified to be slightly smaller compared to the hybrid specimens without separating layer.

#### 4.4. Characterization of the two kinds of impactors – bullets and bearing balls

As briefly described in Section 3.4 the high velocity impact loads on the single specimens of the two different kinds of investigated layups have been applied by two different kinds of impactors. For the first set of specimens commercially available bullets have been used as impactors, whereas for the second set of specimens bearing balls accelerated with weighted propellant in a sabot have been used as impactors. In the following the geometry of the impactor before and after penetration of the material of the specimens is considered. This property is an indicator for the general experimental conditions.

Figure 7 exemplarily illustrates the general mechanical behaviour of the two different kinds of impactors after penetration of the specimen. The photographic pictures on the left (a) show two different views on the distinctly deformed bullets of the kind 9 mm Luger [12]. The high-speed image on the right (b) shows the bulking of the plastic sabot after having left the barrel whereas the bearing ball [11] continues its undisturbed ballistic flight.

The commercially available bullets exhibit distinct plastic deformation after having penetrated the material of the specimens. The two exemplarily shown bullets additionally illustrate a varying deviation in the behaviour of the plastic deformation. The different behaviour could be lead back to the sensitivity of the bullets to the angle of incidence as a significant parameter of the experimental investigations. Thus, for a further evaluation of the results it is not possible to consider only nominal geometrical dimensions of the bullets of the kind 9 mm Luger [12]. The presumed sensitivity to the angle of incidence can then directly be identified as the reason for the slightly higher standard deviations of the results of the first set of the investigated kinds of layups illustrated in Figure 3a and Figure 4a. Additionally the different states of deformation of the impactors are an indicator that the initial energy  $E_{kin,1}$  according to equation (1) and listed in Table 2 for the first set of investigated kinds of layups gets not only dissipated by the material of the specimens but also by the plastic deformation of the impactor in small but statistically varying amounts.

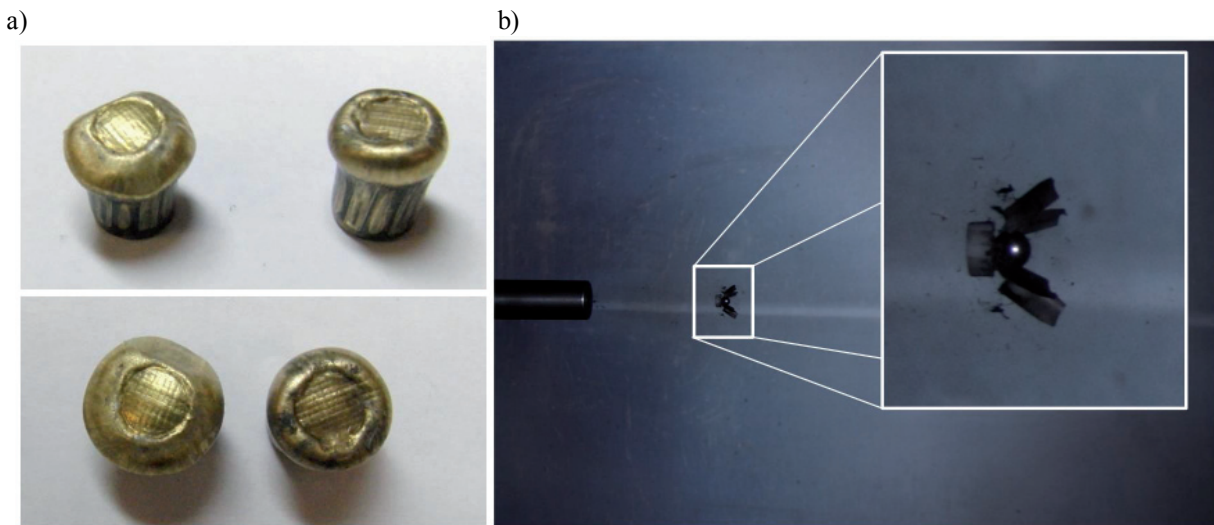


Fig. 7. Photographic pictures of different views on the distinctly deformed bullets of the kind 9 mm Luger [12] (a) and high-speed image of the bulking of the plastic sabot after having left the barrel whereas the bearing ball continues its undisturbed ballistic flight (b)

In contrast to the plastic deformation of the bullets the bearing balls [11] do not exhibit any recognizable deformation after having penetrated the material of the specimens. The bearing ball as an impactor itself hardly deforms and behaves nearly inelastic. Due to the spherical geometry of the bearing ball it is per se insensitive to a possible angle of incidence the lower standard deviations, illustrated in Figure 3b and Figure 4b, can be lead back to this geometric property as well as to the nearly completely inelastic behaviour. This is an indicator that the initial energy  $E_{kin,1}$  according to equation (1) and listed in Table 2 for the second set of investigated kinds of layups gets nearly completely dissipated by the material of the specimens and not by the bearing ball as an impactor.

The identification of spherical bearing balls as insensitive to variations in the angle of incidence has analogously been made e.g. by Muhi, Najim and Moura 2009 [9]. Therein it is additionally observed that the selected spheric geometry provides more reasonable values for the energy dissipation properties when the experimental results are evaluated further or described analytically or numerically [9]. In contrast cylindrical blunt-ended and conical impactors are investigated. Both geometries are assumed to cause distinct stress peaks in the material of the specimen. The main reason therefore is identified as variations of the angle of incidence caused by statistic deviations.

In case of the first set of investigated kinds of layups impacted with bullets the visible delaminated area is

generally very large as it can exemplarily be seen in Figure 5 for the glass fibre reinforced specimen. In contrast in the case of the second set of investigated kinds of layups impacted with bearing balls the visible delaminated area is considerably smaller than the free part of the specimen in the test panel mounting as it can exemplarily be seen in Figure 6 again for the glass fibre reinforced specimen. This observation allows the assumption that the boundary conditions are not completely negligible in case of using bullets as impactors. In contrast, the boundary conditions can be considered negligible in the case of using bearing balls as an impactor.

## 5. Conclusions and outlook

For all evaluated results the standard deviations are generally low. This is an indicator for constant material quality for all the investigated test panels provided by the manufacturing process as well as for the high reproducibility of the experimental investigations of high velocity impact loads. Yet, the standard deviations are slightly higher regarding the evaluated results of the first set of the investigated kinds of layups impacted with bullets. The insensitivity of spherical bearing balls as impactors to the angle of incidence is identified as the main reason for the lower standard deviations regarding the evaluated results of the second set of investigated kinds of layups.

In both cases of the investigated kinds of layups the carried out high velocity impact tests showed the respective properties of each single kind of fibre when the monolithic layups have been considered. With a hybrid stacking it is possible to optimize the use of the outstanding material properties of each single kind of reinforcement fibres when energy dissipation issues under high velocity impact loads are considered. Even though aramid fibres have not been considered as for example described in Muhi, Najim and Moura 2009 [9] hybridization yields noticeable effects. The reasons therefore are the relatively high values of the fibre volume content  $\varphi_{f,e} \approx 60\%$  and at the same time the relatively low standard deviations. These two indicators regarding the composite material imply a high mechanical quality as well as a high degree of reproducibility of the process at the same time. However, aramid fibres should be taken into account in further investigations as even a more distinct enhancement of the energy dissipation capacity can be expected.

The initially described idea to enhance transversal deflection due to shear effects and therewith to enhance the resulting normal loads in the material can be identified in the evaluated results for the hybrid stacked materials with and without the hexagonal separating layers when the evaluated results of the second set of investigated kinds of layups is considered. The improved relative energy dissipation based on the nominal values as well as standardized to the desired fibre volume content distinctly proves the acting of the aimed structural mechanic effect. Thus, besides the functional capability of the hybrid stacked layups as well as the functional capability of the additional separating layer can be stated. In further investigations different hybrid layups should be considered additionally. Thereby the focus should lie on the identification of the sensitivity of the energy dissipation properties to the sequential arrangement of the monolithic blocks in the construction of the hybrid stacked layups as basically carried out in Muhi, Najim and Moura 2009 [9].

Comparing the two kinds of impactors, namely bullets and bearing balls, the bearing balls have been identified to be more suitable for further evaluation of the obtained experimental results. In contrast to the bullets the bearing balls behave nearly inelastic and do not plastically deform due to the penetration of the material of the specimens. Because of their insensitivity to the angle of incidence due to their spherical geometry, the evaluated energy dissipation capacity can directly be addressed to the material properties of the specimen. This fact yields lower standard deviations in the evaluation of the experimental results when bearing balls are used as an impactor. The boundary conditions can

be considered negligible in the case of using bearing balls as an impactor because the delaminated area is considerably smaller than the free part of the specimen.

## Acknowledgements

The authors would like to thank Mr Marco Vogelsberg and Mr Uwe Riedel from the Laboratory of Ballistics, Weaponry and Munitions at the University of the Bundeswehr Munich as well as Mr Florian Roidl from the Laboratory of Manufacturing Engineering and Machine Tools (LFW) and Mr Bastian Jungbauer, B.Eng. from the Laboratory of Composite Technology (LFT), both at the Ostbayerische Technische Hochschule Regensburg.

Further Mrs Carmen Löpelt and Mr Elmar Lauterborn, both from the Wehrwissenschaftliches Institut für Werk- und Betriebsstoffe (WIWeB) Erding are gratefully acknowledged for carrying out the determination of the fibre volume content by chemical extraction.

The authors are grateful to the donation of the bearing balls from the company Schaeffler Technologies AG & Co. KG that have exhibited excellent properties as spheric impactors.

## References

- [1] B.M. Fadhel, Numerically Study of Ballistic Impact of Polycarbonate, Proceedings of the International Symposium "Humanities, Science and Engineering Research" SHUSER, Kuala Lumpur, 2011, 101-105.
- [2] T. Holmquist, G. Johnson, Characterization and evaluation of silicon carbide for high-velocity impact, *Journal of Applied Physics* 97 (2005) 1-12.
- [3] T. Holmquist, G. Johnson, Response of silicon carbide to high velocity impact, *Journal of Applied Physics* 91/9 (2002) 5858-5866.
- [4] R. Jones, *Mechanics of Composite Materials*, Taylor & Francis Group, New York, NY, 1999.
- [5] M. Maier, Experimentelle Untersuchung und numerische Simulation des Crashverhaltens von Faserverbundwerkstoffen. Dissertation, Universität Kaiserslautern, Ludwigshafen, 1990.
- [6] J. Melo, J. Villena, Effect of fiber volume fraction on the energy absorption capacity of composite materials, *Journal of Reinforced Plastics and Composites* 31/3 (2012) 153-161.
- [7] H. Morita, T. Adachi, Y. Tateishi, H. Matsumot, Characterization of impact damage resistance of

- CF/PEEK and CF/Toughened epoxy laminates under low and high velocity impact tests, *Journal of Reinforced Plastics and Composites* 16/2 (1997) 131-143.
- [8] S.S. Morye, P.J. Hine, R.A. Duckett, D.J. Carr, I.M. Ward, Modelling of the energy absorption by polymer composites upon ballistic impact, *Composites Science and Technology* 60/14 (2000) 2631-2642.
- [9] R.J. Muhi, F. Najim, M.F.S.F. de Moura, The effect of hybridization on the GFRP behavior under high velocity impact, *Composites B* 40 (2009) 798-803.
- [10] Basalt fabric BBK.2/2.345.100.12 – Twill weave 2/2. Technical data sheet, Incotology Limited, Pulheim, Germany, 2013.
- [11] Bearing ball. Technical data sheet, Schaeffler Technologies AG & Co. KG, Herzogenaurach, Germany, 2012.
- [12] Bullet 9 mm Luger 8.0 g. Technical data sheet, RUAG Ammotec, Fürth, Germany, 2013.
- [13] Carbon fabric twill weave 2/2. Technical data sheet, ECC – Engineered Cramer Composites, Heek, Germany, 2013.
- [14] DIN 65561 Luft- und Raumfahrt; Faserverstärkte Kunststoffe, Prüfung von multidirektionalen Laminaten, Bestimmung der Druckfestigkeit nach Schlagbeanspruchung, German standard, Beuth Verlag, Berlin/Heidelberg/New York, 1991.
- [15] DIN EN ISO 1172 Textilglasverstärkte Kunststoffe; Prepregs, Formmassen und Laminat; Bestimmung des Textilglas- und Mineralfüllstoffgehalts, German standard, Beuth Verlag, Berlin, 1998.
- [16] DIN EN 2564 Luft- und Raumfahrt; Kohlenstofffaser-Laminat, Bestimmung der Faser-, Harz- und Porenanteile, German standard, Beuth Verlag, Berlin, 1998.
- [17] Epikote Resin 04572 – Anhydrid 180 °C warm curing epoxy resin. Technical data sheet, Momentive, Columbus, OH, USA, 2011.
- [18] Epikote Resin 05128 – Medium viscous 120°C bisphenol A epoxy resin. Technical data sheet, Momentive, Columbus, OH, USA, 2010.
- [19] Glass fabric Interglas Type 92125 – Twill weave 2/2. Technical data sheet, P-D Interglas Technologies GmbH, Erbach, Germany, 2013.
- [20] Lantor Soric XF. Technical data sheet, Lantor BV, Veenendaal, Netherlands, 2013.
- [21] Polyoxymethylen (POM). Technical data sheet, Siegle, Augsburg, Germany, 2013.
- [22] Z. Rosenberg, E. Dekel, Terminal Ballistics. Springer-Verlag, Berlin/Heidelberg/London/New York, 2012.
- [23] V. Schmid, B. Jungbauer, M. Romano, I. Ehrlich, N. Gebbeken, Diminution of mass of different types of fibre reinforcements due to thermal load, Proceedings of the Applied Research Conference, Nürnberg, 2012, in: J. Mottok, O. Ziemann, (Eds.), Applied Research Conference 2012 – ARC 2012, Shaker Verlag, Aachen/Herzogenrath, 2012, 231-235.
- [24] H. Schürmann, Konstruieren mit Faser-Kunststoff-Verbunden, Springer-Verlag, Berlin/Heidelberg, 2005.
- [25] E. Witten, Handbuch Faserverbundkunststoffe, Grundlagen Verarbeitung Anwendungen, GWV Fachverlag, Wiesbaden, 2010.